

Glass transition and crystallization process of hard magnetic bulk $\text{Nd}_{60}\text{Al}_{10}\text{Fe}_{20}\text{Co}_{10}$ metallic glass

WEI Bingchen (魏炳忱)¹, WANG Weihua (汪卫华)^{1,2},
ZHAO Deqian (赵德乾)², ZHANG Yong (张勇)², WEN Ping (闻平)²,
PAN Mingxiang (潘明祥)² & HU Wenrui (胡文瑞)¹

1. National Microgravity Laboratory, Institute of Mechanics, Chinese Academy of Sciences, Beijing 100080, China;

2. Institute of Physics and Center for Condensed Matter Physics, Chinese Academy of Sciences, Beijing 100080, China

Correspondence should be addressed to Wei Bingchen (email: weibc@imech.ac.cn)

Received November 23, 2000

Abstract Glass transition and crystallization process of bulk $\text{Nd}_{60}\text{Al}_{10}\text{Fe}_{20}\text{Co}_{10}$ metallic glass were investigated by means of dynamic mechanical thermal analysis (DMTA), differential scanning calorimetry (DSC), X-ray diffraction (XRD) and scanning electronic microscopy (SEM). It is shown that the glass transition and onset crystallization temperature determined by DMTA at a heating rate of 0.167 K/s are 480 and 588 K respectively. The crystallization process of the metallic glass is concluded as follows: amorphous $\alpha \rightarrow \alpha'$ + metastable FeNdAl novel phase $\rightarrow \alpha' + \text{primary } \delta \text{ phase} \rightarrow \text{primary } \delta \text{ phase} + \text{eutectic } \delta \text{ phase}$ Nd₃Al phase + Nd₃Co phase. The appearance of hard magnetism in this alloy is ascribed to the presence of amorphous phase with highly relaxed structure. The hard magnetism disappeared after the eutectic crystallization of amorphous phase.

Keywords: metallic glass, glass transition, crystallization, hard magnetic.

A number of new metallic alloys with excellent glass forming ability have been developed in the last ten years, and they permit the formation of large bulky ingots of metallic glass^[1-5]. These new alloys have considerable potential as advanced engineering materials due to their excellent processing capabilities in the undercooled liquid, improved wearing resistance, high strength, good corrosion resistance and especially soft magnetism^[6]. More recently, (Nd,Pr)₆₀-Fe₃₀Al₁₀ metallic glass of a diameter up to 12 mm with high coercivity has been newly reported^[7]. The high coercivity of Nd-Al-Fe based alloys was also observed by Ding et al.^[8]. The hard magnetic Nd-Fe-Al based alloys are of interest in both practical and scientific viewpoints. However, there are only a few works focusing on the glass transition and the crystallization process of these new bulk metallic glass (BMG), although these processes are important in establishing the stability of these glassy materials^[7-9].

In this work, the glass transition temperature and crystallization sequence of a bulk $\text{Nd}_{60}\text{Al}_{10}\text{Fe}_{20}\text{Co}_{10}$ glass are determined and the results will be helpful to understanding the reason for the appearance of hard magnetism in Nd-based BMGs.

1 Experimental procedures

Ingots with compositions of $\text{Nd}_{60}\text{Al}_{10}\text{Fe}_{20}\text{Co}_{10}$ were prepared by arc melting from elemental

Nd, Fe, Al and Co with a purity of 99.9% in a titanium-gettered argon atmosphere. Cylindrical specimens of 3 mm in diameter and 50 mm in length were prepared from the ingots by die casting into a copper mold under argon atmosphere. The structure of the as-cast cylinder was characterized by XRD in a Siemens D5000 diffractometer using Cu K α radiation. Thermal analysis was performed using a Perkin-Elmer DSC-7 differential scanning calorimeter under argon atmosphere. A heating rate of 0.17 K/s was applied. The dynamic mechanical properties were measured by a dynamic mechanical thermal analyzer (DMTA IV). Microstructure was studied by a Cambridge scanning electron microscope (SEM) equipped with Link energy dispersive X-ray (EDX) microanalysis system. Magnetic measurements were performed using vibrating sample magnetometer (VSM) with a maximum applied field of 1592 kA/m.

A dynamic mechanical investigation can be performed by applying a sinusoidal stress $\sigma(t) = \sigma_0 \sin(\omega t)$ at frequency ω . A deformation $\epsilon(t) = \epsilon_0 \sin(\omega t - \delta)$ is then observed with phase shift σ . The in-phase answer of the system is related frequency to the dependent Young's storage modulus $E'(\omega)$, which describes the cycled elastic energy of the system, while the out-of-phase answer is related also to the frequency dependent Young's loss modulus $E''(\omega)$, which describes the energy dissipated in every cycle. They are determined by $E'(\omega) = \frac{\sigma_0}{\epsilon_0} \cos \delta$, and $E''(\omega) = \frac{\sigma_0}{\epsilon_0} \sin \delta$. Introducing complex notation $\sigma^*(t) = \sigma_0 \exp(i\omega t)$ and $\epsilon^*(t) = \epsilon_0 \exp[i\omega t - \delta]$, a complex Young's modulus $E^*(\omega)$ can be defined by $E^* = \frac{\sigma(t)}{\epsilon(t)} = \left(\frac{\sigma_0}{\epsilon_0} \right) \exp(i\delta) = \left(\frac{\sigma_0}{\epsilon_0} \right) (\cos \delta + i \sin \delta) = E' + iE''$. Thus, the storage modulus is represented by the real part, and the loss modulus is represented by the imaginary part of the complex modulus. Generally, the complex modulus is calculated by $E = |E^*| = \sqrt{E'^2 + E''^2}$. When $E' \gg E''$, the E' can be considered as E^* . In this investigation, the temperature-dependent Young's modulus E was measured with three-point bending samples of 1.2 mm \times 3.0 mm \times 30 mm in dimensions under dynamic conditions with a static load of 1 N at a frequency of 1 Hz.

2 Results

Fig. 1 shows the hysteresis M - H loop of the bulk Nd₆₀Al₁₀Fe₂₀Co₁₀ metallic glass. It can be seen that the as-cast sample exhibits hard magnetism at room temperature with a coercivity of 326 kA/m. The Curie temperature of the sample is about 450 K measured by VSM. These values are in agreement with the results of Inoue and Ding et al. on the Nd based BMG^[7, 8].

DSC curve of the as-cast Nd₆₀Al₁₀Fe₂₀Co₁₀ BMG is shown in fig. 2. It exhibits two exothermic reactions, a lower temperature weak peak ranging from 638—763 K and a higher temperature sharp peak, followed by an endothermic reaction of melting. The obvious endothermic peak due to the glass transition is not observed in the trace, and this result is consistent with Inoue and Jing et al.'s results on NdFeAl based alloys^[7, 8]. The sharp exothermic peak is obviously caused by crystallization reaction, while the origin of the weak exothermic peak is still unclear. The glass transition and onset crystallization temperature cannot be determined by the generally accepted DSC method.

Dynamic mechanical thermal analysis on the as-cast sample is shown in fig. 3. Starting from

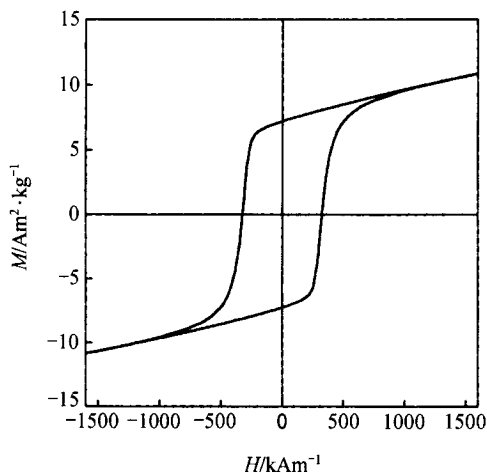


Fig. 1. Hysteresis loop for $\text{Nd}_{60}\text{Al}_{10}\text{Fe}_{20}\text{Co}_{10}$ BMG at room temperature.

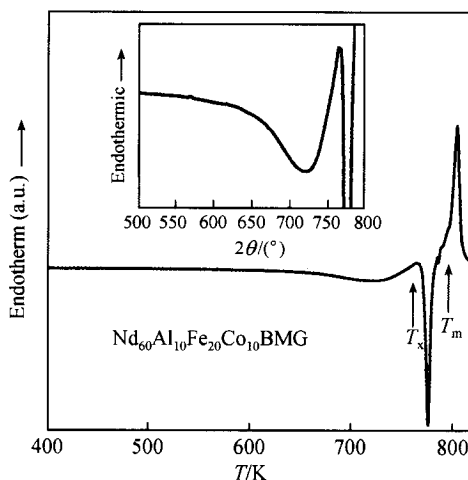


Fig. 2. DSC curve for the as-cast $\text{Nd}_{60}\text{Al}_{10}\text{Fe}_{20}\text{Co}_{10}$ BMG.

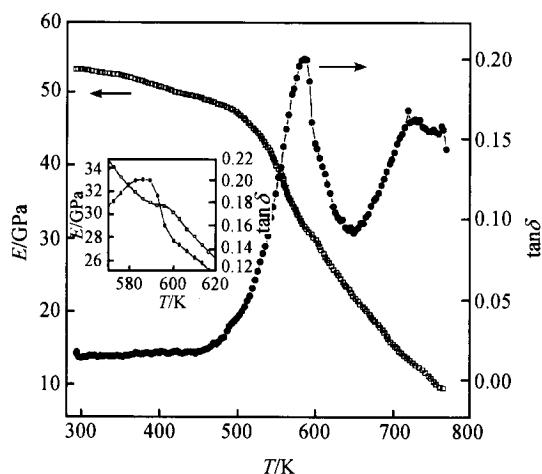


Fig. 3. Temperature dependence of Young's modulus and loss angle for $\text{Nd}_{60}\text{Al}_{10}\text{Fe}_{20}\text{Co}_{10}$ BMG. ●, $\tan\delta$; □, E .

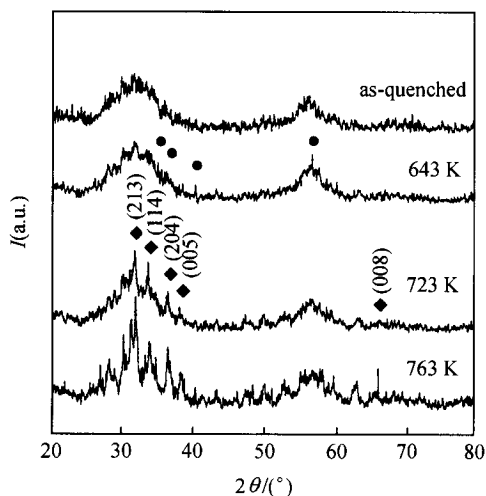


Fig. 4. Results of XRD for $\text{Nd}_{60}\text{Al}_{10}\text{Fe}_{20}\text{Co}_{10}$ annealed at different temperatures for 1.8 ks. ●, Metastable phase; ◆, δ phase.

room temperature, Young's modulus E decreases slightly as expected for conventional metals, then the specimen softens rapidly at temperature about 493 K. The corresponding $\tan\delta$ curve shows a large loss of energy above 493 K. With further increasing temperature, the E value shows a weak peak with an onset temperature of 590 K, and the corresponding $\tan\delta$ shows a sharp peak. Subsequently, the $\tan\delta$ value decreases steeply. In the temperature range from 638–763 K, the $\tan\delta$ curve shows a broad peak.

The XRD results of the isothermal annealed $\text{Nd}_{60}\text{Al}_{10}\text{Fe}_{20}\text{Co}_{10}$ are shown in fig. 4. Annealing at 643 K for 1.8 ks results in the appearance of unknown metastable phases, which transform into an equilibrium phase after annealing at 723 K. Further annealing at 763 K leads to precipita-

tion of more equilibrium phases. The back scattering electron (BSE) image shows that this phase is dark, rod-like grain with a Fe:Nd:Al ratio of 75:16:9 as shown in fig. 5(a). The chemical content and XRD pattern show that it is a novel phase. Its structure and magnetic properties are just under investigation. After annealing at 723 K, the BSE results show that the rod-like metastable phase disappeared. Instead, a plate-like stable phase is distributed in the remains amorphous matrix as shown in fig. 5(b). The EDX results show that this phase contains less Fe, and its Fe:Nd:Al ratio is 49:34:17. This composition is close to the composition range of $\delta(\text{Fe}_{67.5-x}\text{Al}_x\text{Nd}_{32.5}, 7 < x < 25)$ phase, which is hexagonal with antiferromagnetism^[9,10]. The XRD results in fig. 4 confirm the hexagonal structure of δ phase. The BSE image of the $\text{Nd}_{60}\text{Al}_{10}\text{Fe}_{20}\text{Co}_{10}$ further annealed at 763 K shows that the structure consists of primary δ plus inter-phase eutectic phases as shown in fig. 5(c). The EDX results show that the eutectic consists of the thin plate-like eutectic δ , dark Nd_3Al (hexagonal), and bright Nd_3Co (orthorhombic). This structure is similar to the ternary NdAlFe eutectic except for $\alpha\text{-Nd}$ replaced by Nd_3Co ^[9,11].



Fig. 5. BSE image for $\text{Nd}_{60}\text{Al}_{10}\text{Fe}_{20}\text{Co}_{10}$ annealed at 643 K (a), 723 K (b) and 763 K (c) for 1.8 ks.

The dependence of H_c , M_s and M_r on isothermal annealing temperature for $\text{Nd}_{60}\text{Al}_{10}\text{Fe}_{20}\text{Co}_{10}$ alloy is shown in fig. 6. The results show that the hard magnetic properties remain almost unchanged in the annealing temperature ranging up to 743 K below the eutectic crystallization temperature determined by the above analysis.

3 Analysis and discussion

3.1 Glass transition and crystallization sequence

The previous studies of Chen et al.^[12] on dynamic mechanical properties of metallic glass show that the mechanical properties change greatly near the glass transition temperature. Rambousky et al.^[13] pointed out that the glass transition temperatures measured by dynamic mechanical analysis agree well with the DSC results.

In our DMTA result of $\text{Nd}_{60}\text{Al}_{10}\text{Fe}_{20}\text{Co}_{10}$ BMG, Young's modulus E decreases rapidly at about 480 K, and the corresponding $\tan\delta$ value increases continually in the temperature range from 480—588 K, which is much higher than the Curie temperature of the as-cast sample. This indicates that the remarkable softening of sample is not caused by the magnetic transition of this hard magnetic BMG. Moreover, the high $\tan\delta$ value also reveals that this transition is not a low temperature relaxation process. Consequently, this remarkable transition is believed to be glass

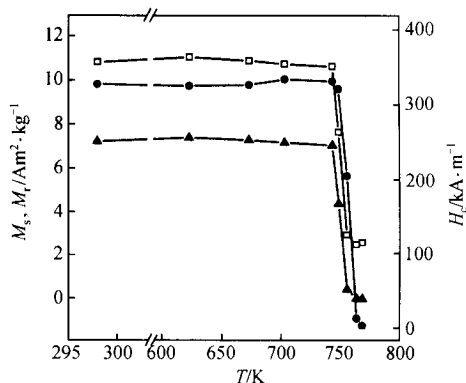


Fig. 6. Dependence of H_c (\bullet), M_s (\square) and M_r (\blacktriangle) on isothermal annealing temperature for $\text{Nd}_{60}\text{Al}_{10}\text{Fe}_{20}\text{Co}_{10}$ alloy (1.8 ks).

transition. This remarkable decrease of E was also observed at glass transition temperature in Zr- and La-based BMG^[13,14]. With further increase of temperature, E value attains a weak peak at around 600 K. The corresponding $\tan\delta$ value attains a sharp peak at 588 K, then decreases greatly. This suggests that a certain crystalline phase precipitates from the amorphous matrix. The XRD and SEM results confirm the precipitation of the crystalline phase, which is proved to be a novel metastable FeNdAl ternary phase, with the composition near Fe₇₅Nd₁₆Al₉. The T_g and T_{x1} temperature determined by DMTA result are 480 and 588 K respectively, and the melting temperature is 792 K. Thus, the reduced glass transition temperature ($T_{rg} = T_g/T_m$) is calculated to be 0.61, and the supercooled liquid region ($\Delta T_x = T_{x1} - T_g$) is 108 K. The large value of T_{rg} and ΔT_x of this alloy is in consistent with its good glass forming ability.

The broad peak from 638—763 K in $\tan\delta$ curve corresponds to the broad exothermal reaction in DSC curve. The E curve has no obvious change in slope in this temperature range. This shows that the exothermic reaction does not change the Young's modulus very much. The XRD and SEM results show that the metastable FeNdAl ternary phase disappears after annealing at 723 K, and an equilibrium phase precipitates. The above results indicate that the broad peak in DSC and DMTA curves is caused by the transition from metastable phase to equilibrium phase and the growth of the equilibrium phase. From the SEM and XRD results, we can see that the remaining amorphous phase between primary δ phase crystallizes into eutectic $\delta + \text{Nd}_3\text{Co} + \text{Nd}_3\text{Al}$ after annealing at 763 K. So the sharp exothermic peak in DSC curve is caused by the eutectic crystallization of remaining amorphous phase.

3.2 Hard magnetism

The dependence of H_c , M_s and M_r on isothermal annealing temperature for Nd₆₀Al₁₀Fe₂₀Co₁₀ alloy shows that the precipitation and growth of the novel metastable FeNdAl phase and the primary δ -FeNdAl phase have no significant effect on the magnetic properties of the BMG. The BMG maintains the hard magnetism up to the eutectic crystallization of remaining amorphous phase. The δ phase is antiferromagnetic, and the magnetic properties of the metastable FeNdAl are thought to be antiferromagnetic or paramagnetic. The magnetic measurement results show that high coercivity in the NdAlFeCo alloy is due to the presence of the amorphous phase. The hard magnetism disappears after the completely crystallization of the amorphous phase.

Our results support the previously proposed ferromagnetic cluster model with large random anisotropy^[15]. It has been reported that binary Nd-Fe amorphous alloy ribbons prepared by melt spinning exhibit ferromagnetism and that the coercivity at room temperature increases with increasing Nd content and shows a maximum value of about 150 kA/m at 40% Nd. The high coercivity is explained by the ferromagnetic cluster model; that is, the amorphous Nd-Fe alloy can be regarded as an ensemble of clusters composed of Fe and Nd atoms, and the high coercivity of the homogeneous magnetic system has been presumed to result from the magnetic exchange coupling interaction among the clusters with large local magnetic anisotropy. In our investigation the high coercivity is attributed to the development of the homogeneous dispersion of the Nd-Fe and Nd-Co clusters with large local magnetic anisotropy from the highly relaxed disordered structure. The present Nd₆₀Al₁₀Fe₂₀Co₁₀ BMG solidified more slowly than the melt-spun Nd-Fe ribbons. Medium-range atomic rearrangements may occur during solidification. Hence, atomic clusters with higher degree of short-range order may be formed in the BMG. The BMG has higher degree of exchange coupling between clusters, and exhibits higher coercivity. That no obvious low tempera-

ture relaxation reaction is detected in the DSC and DMTA measurement in this work confirms the highly relaxed structure of the BMG.

4 Conclusions

(i) The glass transition temperature and onset crystallization temperature determined by DMTA method at a heating rate of 10 K/s are 480 and 588 K respectively. The calculated reduced glass transition temperature and supercooled liquid region are 0.61 and 108 K respectively.

(ii) The crystallization process of this BMG is concluded as follows: amorphous $\alpha \rightarrow \alpha' +$ metastable FeNdAl phase $\rightarrow \alpha' +$ primary δ -FeNdAl phase \rightarrow primary δ phase + eutectic δ phase + Nd₃Al + Nd₃Co.

(iii) The precipitation and growth of the metastable FeNdAl and the primary δ phase have no significant effect on the magnetic properties of the Nd₆₀Al₁₀Fe₂₀Co₁₀ glass. The hard magnetism disappears after the eutectic crystallization of the amorphous matrix.

(iv) The presence of amorphous phase with highly relaxed structure is responsible for the appearing of the hard magnetism in Nd₆₀Al₁₀Fe₂₀Co₁₀ alloy.

Acknowledgements The authors would like to thank Prof. M. L. Guo of Beijing University of Aeronautics and Astronautics for her valuable suggestions and help. This work was supported by the National Natural Science Foundation of China (Grant No. 59925101) and the fund of Climbing Program provided by the Ministry of Science and Technology of China (Grant No. 95-yu-34).

References

1. Inoue, A., Zhang, T., Masumoto, T., Production of amorphous cylinder and sheet of La₅₅Al₂₅Ni₂₀ alloy by a metallic mold casting method, *Mater. Trans. JIM*, 1990, 31: 425—428.
2. Inoue, A., Zhang, T., Nishiyama, N. et al., Amorphous Zr-Al-TM (TM = Co, Ni, Cu) alloys with significant supercooled liquid region of over 100 K, *Mater. Trans. JIM*, 1991, 32: 1005—1010.
3. Peker, A., Johnson, W. L., A highly processably metallic glass: Zr_{41.2}Ti_{13.8}Cu_{12.5}Ni_{10.0}Be_{22.5}, *Appl. Phys. Lett.*, 1993, 63: 2342—2344.
4. Lin, X. H., Johnson, W. L., Formation of Ti-Zr-Cu-Ni bulk metallic glasses, *J. Appl. Phys.*, 1995, 78: 6514—6519.
5. Wang, W. H., Wang, W. K., Bai, H. Y., Formation of new Zr-Ti-Cu-Ni-Be-C bulk amorphous alloy, *Science in China, Ser. A*, 1998, 42(7): 756.
6. Inoue, A., Stabilization of metallic supercooled liquid and bulk amorphous alloys, *Acta Mater.*, 2000, 48: 279—306.
7. Inoue, A., Zhang, T., Bulk amorphous alloys with soft and hard magnetic properties, *Mater. Sci. and Eng.*, 1997, A226-228: 357—363.
8. Ding, J., Li, Y., Wang, X. Z., The coercivity of rapidly quenched Nd₆₀Fe₃₀Al₁₀ alloys, *Phys. D: Appl. Phys.*, 1999, 32: 713—716.
9. Grieb, B., Henig, E. T., Martinek, G. et al., Phase relations and magnetic properties of new phases in the Fe-Nd-Al and Fe-Nd-C systems and their influence on magnets, *IEEE Trans. Magn.*, 1990, 26: 1367—1369.
10. Ding, J., Si, L., Li, Y. et al., Magnetoresistivity and metamagnetism of the Nd₃₃Fe₅₀Al₁₇ alloy, *Appl. Phys. Lett.*, 1999, 75: 1763—1765.
11. Pierre, V., Handbook of Ternary Alloy Phase Diagrams, Materials Park, OH: ASM International, 1994, 3525, 3052.
12. Chen, H. S., Morito, N., Sub- $T_g\alpha'$ relaxation in a PdCuSi glass; internal friction measurements, *J. Non-Cryst. Solids*, 1985, 72: 287—299.
13. Rambousky, R., Moske, M., Samwer, K., Dynamic mechanical analysis of ZrAlCu-alloys at and above the glass transition temperature, *Mater. Sci. Forum.*, 1995, 179-181: 761—766.
14. Okumara, H., Chen, H. S., Inoue, A. et al., Structural relaxation of a La₅₅Al₂₅Ni₂₀ amorphous alloy measured by an internal friction method, *Jpn J. Appl. Phys.*, 1991, 30: 2553—2557.
15. Nagayama, K., Ino, H., Sato, N. et al., Magnetic properties of amorphous Fe-Nd alloys, *J. Phys. Soc. Jpn.*, 1990, 59: 2483—2495.